

Supplementary information

All-Gas-Phase Preparation of Organic/Inorganic Heterolayered Multifunctional
Electrodes for Hybrid-Type Energy Storage

*Minseong Ju,^b Changjun Kim,^b Jisun Lee,^b Sangmin Kim,^b Thi Thuong Thuong Nguyen,^b
Cuong Van Le,^b Haney Lee,^b Mincheol Chang^{a,b} and Hyeonseok Yoon^{a,b*}*

^aSchool of Polymer Science and Engineering, Chonnam National University, 77 Yongbong-ro,
Buk-gu, Gwangju 61186, South Korea.

E-mail: hyoon@chonnam.ac.kr; Fax: +82-62-530-1779; Tel: +82-62-530-1778

^bDepartment of Polymer Engineering, Graduate School, Chonnam National University,
77 Yongbong-ro, Buk-gu, Gwangju 61186, South Korea

Corresponding author:

*E-mail: hyoon@chonnam.ac.kr

Keywords: Conducting polymers; 2D materials; Nanohybrids; Electrode materials; Energy storage
devices

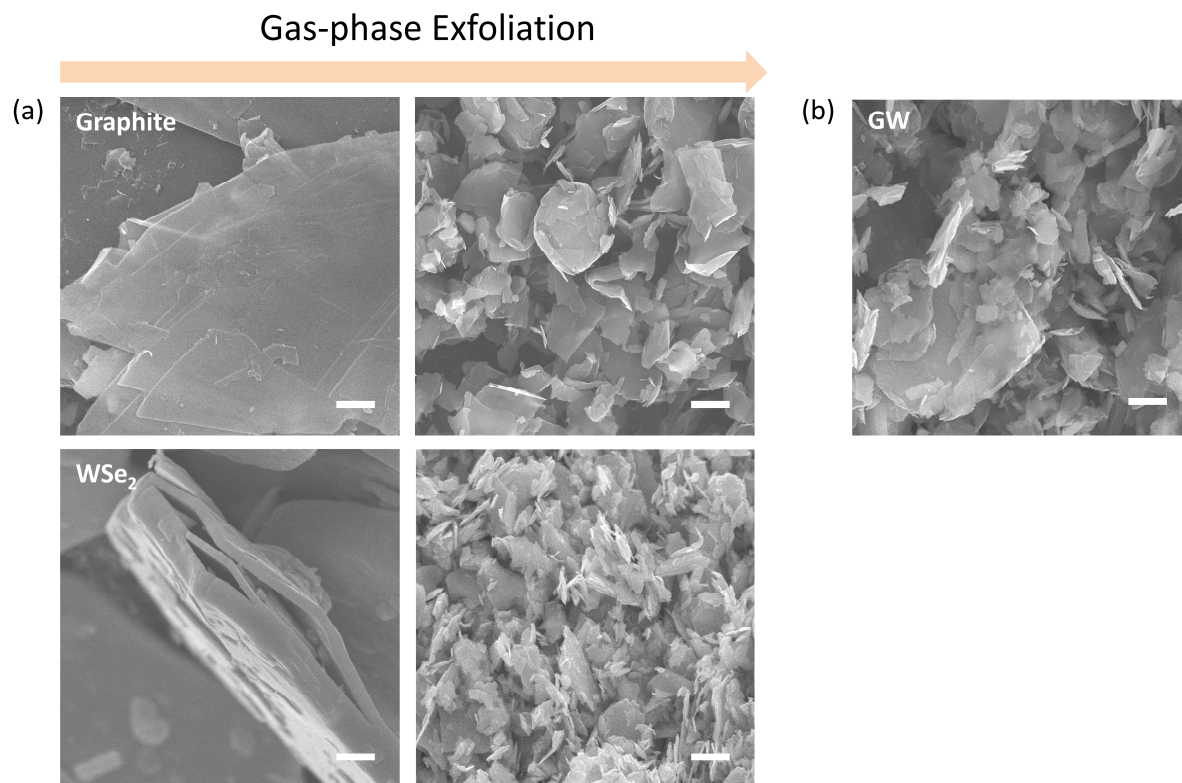


Figure S1. SEM images of (a) bulk sheets (left) and gas-phase exfoliated nanosheets (right) for graphite and WSe₂ (scale bar: 1 μm), and (b) GW nanohybrids (scale bar: 1 μm). G: graphite; W: WSe₂.

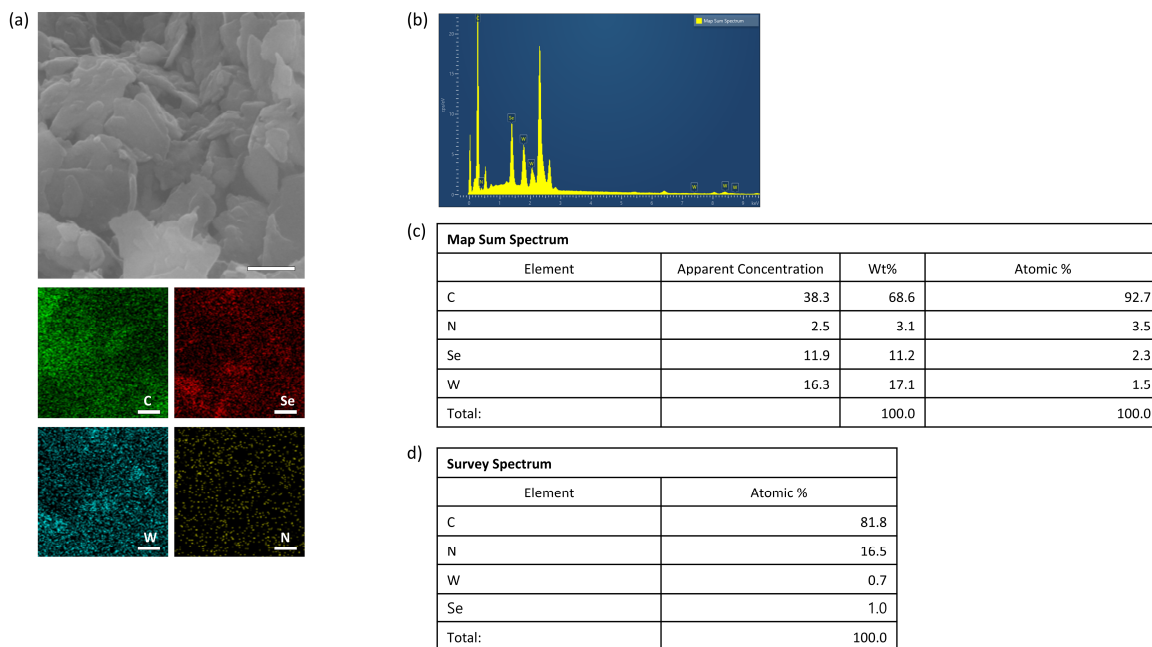


Figure S2. (a) SEM image and corresponding energy-dispersive X-ray spectroscopy elemental mapping images of GWP2 nanohybrids, with each mapping image shown in a different color for a specific element (scale bar: 0.5 μm). (b) Map sum spectrum analysis of the scanned GWP2 specimen. (c) Apparent Concentrations, including weight and atomic percentage, derived from the map sum spectrum. (d) XPS elemental composition in atomic percentage of the constituent elements in GWP2.

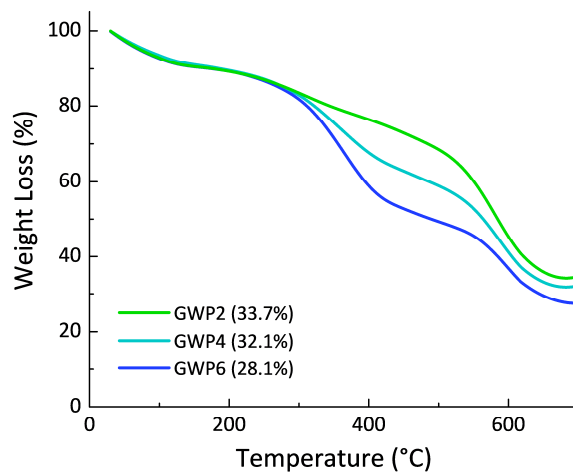


Figure S3. Thermogravimetric analysis curves of the GWPs recorded at a heating rate of $10\text{ }^{\circ}\text{C min}^{-1}$ under a nitrogen atmosphere. Weight percentages of the residues are indicated in the legend.

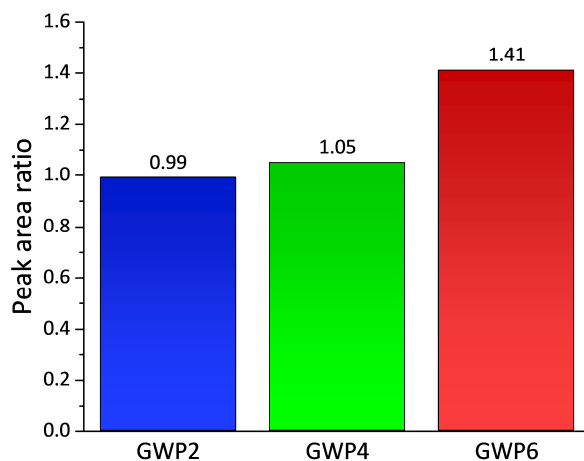


Figure S4. Integrated peak area ratio of WO_3 -to- WSe_2 in GWPs reflecting partial oxidation and p-type doping.

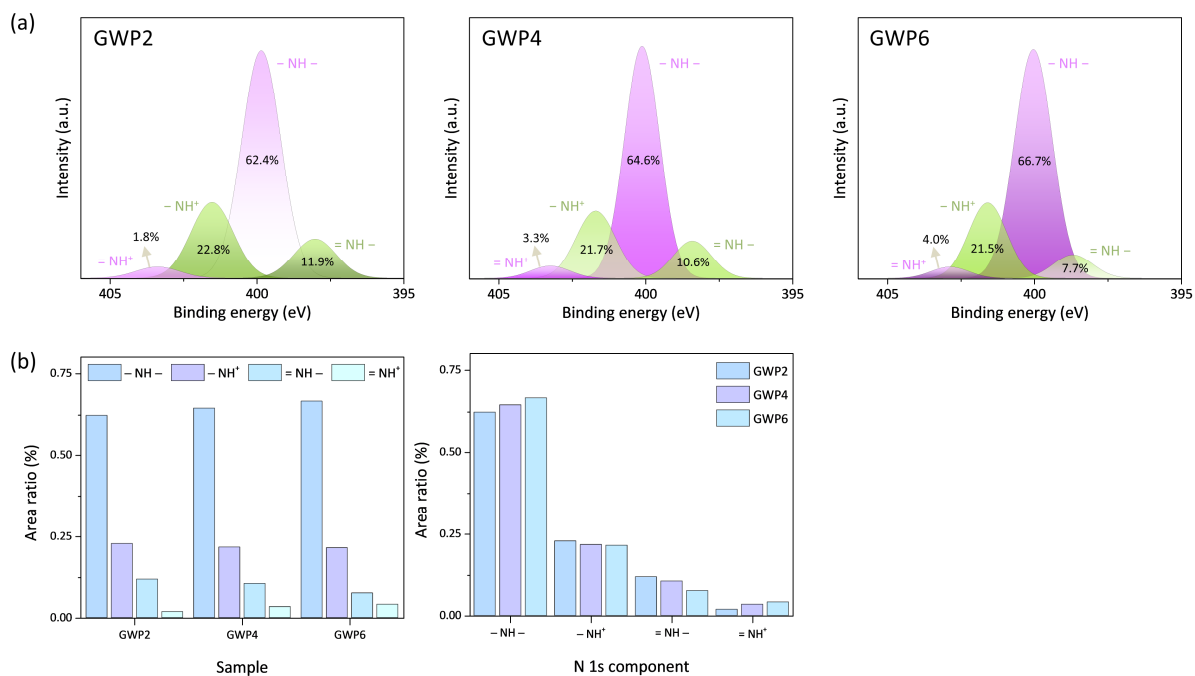


Figure S5. (a) Deconvolution of N 1s high-resolution XPS spectra for GWPs. (b) Area ratios of N 1s components in GWPs (left) and contributions of GWPs to N 1s components (right).

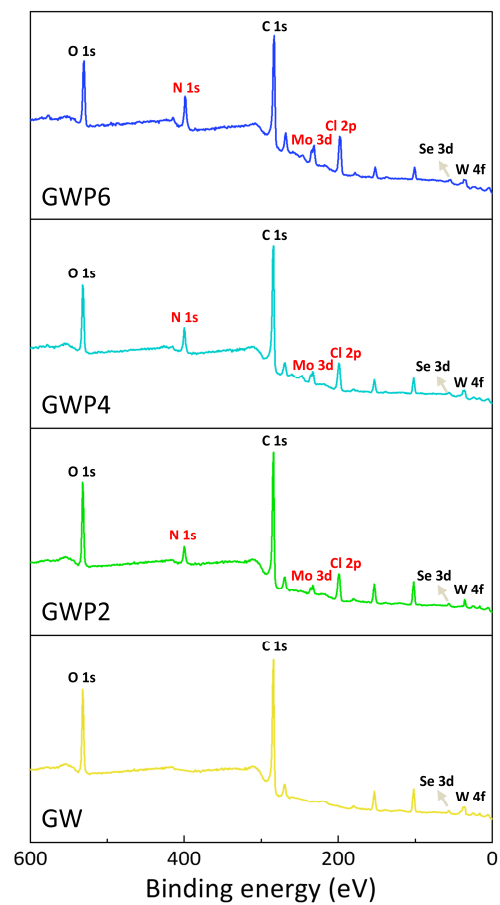


Figure S6. XPS survey scan of the GWPs and control.

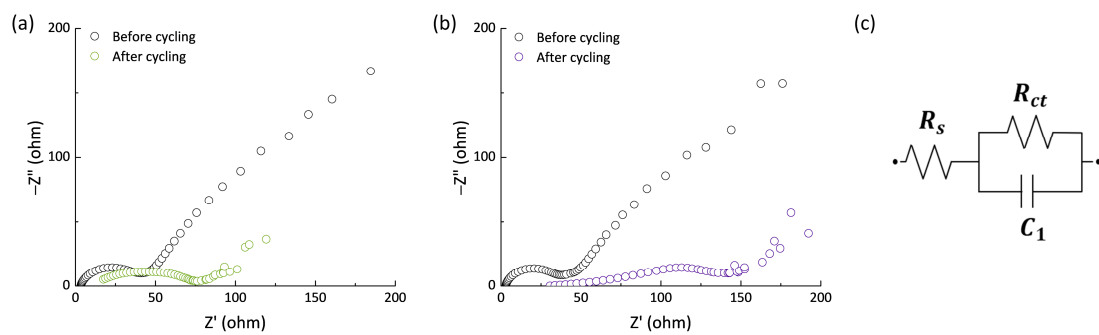


Figure S7. EIS Nyquist plots recorded before and after (a) half-cell and (b) full-cell tests in the frequency range of 100 mHz to 0.1 MHz. (c) Equivalent circuit model used for EIS analysis.

Table S1. Atom labels for corresponding symbols used in model structures.

Atom labels	Symbols
C	
H	
W	
Se	
Mo	
Cl	

Table S2. Charge transfer coefficients calculated for GWPs.

Sample	GWP2	GWP4	GWP6
α	0.227	0.205	0.115

Table S3. Comparison of GWP2-based LHC with previously reported LHCs in terms of energy density, power density, and cycling performance.

Electrode materials	Voltage window (V)	Energy density Wh kg ⁻¹	Power density W kg ⁻¹	Cycling stability	Coulombic efficiency (%)	References
This work	1.0–4.0	256.0	24,461	88% after 3000 cycles at 1 A g ⁻¹	~100%	
NPC//CHPC	0.01–4.2	220.0	6690	70% after 3000 cycles at 2 A g ⁻¹	~100%	47
SnS ₂ /RGO//BCN	0.0–4.5	149.5	35,000	90.5% after 10000 cycles at 5 A g ⁻¹	~100%	48
PDA-GN//PG	0.01–4.2	135.6	21,000		99%	49
Nb ₂ O ₅ @C//MSP-20	1.0–3.5	63.0	16,500	100% after 1000 cycles	~100%	50
ANCS//ANCS	0.0–4.5	206.7	22,500	86.6% after 10000 cycles at 4 A g ⁻¹	~100%	51
MnO/C//CNS	1.0–4.0	100.0	20,000	97.3% after 10000 cycles at 5 A g ⁻¹	~100%	52
Sn-NP-CNF//AC	0.01–4.0	186.0	20,000	83.7% after 10000 cycles at 5 A g ⁻¹	~100%	53
NPG//AC	1.0–4.0	195.0	14,984	98% after 3000 cycles	99%	54